Composites Part B 150 (2018) 1–6

Contents lists available at ScienceDirect

Composites Part B

journal homepage: www.elsevier.com/locate/compositesb

Sustainable nanocomposites of epoxy and silica xerogel synthesized from corn stalk ash: Enhanced thermal and acoustic insulation performance

Gulcihan Guzel Kaya, Elif Yilmaz, Huseyin Deveci*

Department of Chemical Engineering, Faculty of Engineering, Selcuk University, Konya, 42075, Turkey

ARTICLE INFO

Keywords:
Nano-structures
Polymer-matrix composites (PMCs)
Thermosetting resin
Thermal properties

ABSTRACT

The synthesis of silica xerogel from corn stalk ash in ambient pressure drying was carried out by sol-gel method. With the usage of silica xerogel (0.5, 1.0 and 1.5 wt%) in epoxy resin (ER), silica xerogel/epoxy nanocomposites were successfully prepared. The uniform dispersion of silica xerogel in neat ER was observed except nanocomposite including 1.5 wt% silica xerogel. The low density nanocomposites showed high thermal stability and low thermal conductivity. The char residue at 600 °C and thermal conductivity of nanocomposite including 1.5 wt% silica xerogel were specified as 20.30% and 0.220 W/mK, respectively. The acoustic velocity of the nanocomposites was decreased with increasing amount of silica xerogel. The water sorption of the nanocomposites was slightly higher than neat ER. The water contact angle of the nanocomposites were between 75° and 70°. The study provided a new thermal and acoustic insulation material instead of expensive and health risk traditional materials.

1. Introduction

The United Nation Environment Program forecasts that the buildings use up approximately 40% of the world global energy, 40% of the global resources and 25% of the global water [1]. And also, the buildings account for more than 30% of the greenhouse gas emissions in many countries [2]. Energy saving thermal insulation materials have attracted a great deal of attention due to the increasing significance of environmental issues in the recent years. Traditional thermal insulation materials such as mineral wool, glass wool, foam glass, expanded polystyrene, extruded polystyrene, phenolic resin foam and polyurethane foam have been used in many applications [3,4]. State-of-the-art thermal insulation materials including vacuum insulation panels, gas-filled panels, aerogels and phase change materials come into prominence with the advantages of space saving, long service life, great thermal performance and high resistance to water and chemicals, lately [5]. At the same time, noise pollution resulted from living activities, railway, urban and highway road traffic, factories etc. is a serious problem all over the world. Nowadays, concrete block, brick, glass, wood, glass wool, foam are generally preferred to decrease sound transmission [6–8].

Silica aerogels are high-performance insulation materials owing to high porosity (~99%), ultralow density (~1 kg/m^3), low thermal conductivity (0.01 W/mK) and low sound speed (< 70 m/s) [9,10]. The silica aerogels have potential by the help of desirable thermal and acoustic properties in many applications such as buildings, roofs, refrigerators, refrigerated vehicles, space crafts, vessels, automotive exhaust pipes and so on [11–13]. However, expensive raw materials and complicated drying process with super critical fluids restrict utilization of silica aerogels. Instead of silica aerogels, investigations about synthesis of low cost and environmentally friendly silica xerogels with using inorganic/organic materials or agricultural wastes at ambient pressure drying conditions have rapidly increased [14]. Up to now, various silica based materials are prepared from fly ash [15], oil shale ash [16], kaolin [17], montmorillonite [18], chitosan [19], cellulose [20], bagasse ash [21], sago waste ash [22], wheat starch [23], rice husk [24] for different purposes in the literature.

Epoxy resins (ERs) are one of the commonly used thermoset polymers in structural adhesives, coatings, laminates, construction materials, composites, insulation materials, aerospace structure materials and so on [25–27]. Their properties such as excellent moisture, chemical and solvent resistance, high mechanical strength, low density, low shrinkage, strong adhesive to different substrates, desirable dielectric constant make the ERs promising materials. In spite of these advantages, thermal properties of ERs must be enhanced especially in field required high thermal stability [28,29].

When considering literature studies, there are limited number of studies related with epoxy nanocomposites including silica xerogel obtained from agricultural waste. In this study, low cost silica xerogel was easily synthesized from corn stalk ash at ambient conditions to be

* Corresponding author.
E-mail address: hdeveci@selcuk.edu.tr (H. Deveci).

https://doi.org/10.1016/j.compositesb.2018.05.039
Received 13 April 2018; Accepted 24 May 2018
Available online 25 May 2018
1359-8368/

used as filler in epoxy nanocomposites for the first time. The hopeful results showed that the obtained mesoporous silica xerogel provided to enhance thermal and acoustic insulation performance of the ER.

2. Experimental section

2.1. Materials

The corn stalk was obtained in dry state from Adana region in Turkey. Sodium hydroxide (NaOH), hydrochloric acid (HCl), isopropanol, n-hexane and distilled water were used in silica xerogel synthesis. Bisphenol A type ER commercially known as NPEL 128 (epoxide equivalent: 184–190 g/eq and viscosity: 12–15 Pa.s at 25 °C) was used as matrix. Methylnadic anhydride and 2,4,6-tris(dimethylaminomethyl) phenol were preferred as hardener and accelerator, respectively.

2.2. Pretreatment of corn stalk

The corn stalk was burned to obtain corn stalk ash (CSA) at 650 °C with a heating rate of 5 °C/min in a furnace for 3 h. Acid washing step with 3 M HCl was carried out at 60 °C for 2 h to remove small quantities of minerals. The slurry was filtered and washed with distilled water until pH 7 [30]. Then, the CSA was dried at 70 °C for 24 h in an oven. The chemical composition of corn stalk ash was approximately SiO_2 49%, CaO 19%, Al_2O_3 9%, MgO 8%, Fe_2O_3 7%, K_2O 4%, MnO_2 2% and Na_2O 2%.

2.3. Synthesis of silica xerogel from CSA

Sol-gel method was efficiently used for synthesis of silica xerogel from CSA. After mixing CSA and 3 M NaOH at a ratio of 1:6 (w/v), the mixture was heated for 5 h at boiling point with constant stirring under reflux. The Na_2SiO_3 solution was filtered and neutralized by 3 M HCl solution until gelation. Subsequently, the silica gel was washed with distilled water at room temperature three times for 4 h each time. In the aging step to strengthen gel network, the silica gel was immersed in water/isopropanol (v/v: 1/1), isopropanol and n-hexane at 50 °C three times during a day, respectively. Finally, the aged gel was dried at 50 °C for 24 h in an oven [31].

2.4. Preparation of silica xerogel/epoxy nanocomposites

The silica xerogels (0.5, 1.0 and 1.5 wt%) and ER were mixed with mechanical stirrer to obtain uniformly dispersed blends for 30 min at room temperature. Removing of entrapped bubbles in each blends and increasing chain mobility to ER were provided by sonication. After adding 30 wt% MNA to blends while stirring, the accelerator was dropped to the each blend. The blends were poured into the mold which was prepared according to the ASTM D 638 Standard. The bubble free blends were cured at 60 °C for 4 h followed by post-curing at 120 °C for 4 h.

2.5. Characterizations

Fourier transform infrared spectroscopy (FTIR) analysis was performed on Bruker Vertex 70 to determine chemical bonding state of silica xerogel in the 4000 - 400 cm^{-1} range. X-ray diffraction (XRD) pattern was recorded for phase analysis of the silica xerogel by Bruker D8 Advance X-ray diffractometer with Cu Kα radiation (λ = 0.154 nm) at 40 kV and 40 mA in the range of 10°–80°. N_2 adsorption-desorption isotherm of silica xerogel was obtained on Micromeritics Tristar II 3020 surface area and porosity analyzer at 77 K, after the samples were degassed at 423 K for 12 h. The surface area, average pore diameter and pore volume were determined using Brunauer-Emmett-Teller (BET) and Barrett-Joyner-Halende (BJH) method, respectively. Scanning electron microscopy (SEM) analyses were carried out to investigate morphology of the silica xerogel and epoxy nanocomposites by SM Zeiss LS-10 scanning electron microscope at 20 kV, after coating surfaces with a fine gold layer. Thermogravimetric analyses (TGA) were employed to examine thermal stability of the silica xerogel and epoxy nanocomposites with METTLER STAR SW thermal analyzer at a heating rate of 10°/min. Thermal conductivity of the silica xerogel and epoxy nanocomposites was measured by C-THERM thermal conductivity analyzer at room temperature. The measurements were repeated three times for each material to get reliable results. The pulse-echo method was used to determine acoustic velocity of the epoxy nanocomposites at room temperature [32]. Ultrasonic pulses were supplied at 20 MHz by PANAMETRICS-NDT ultrasonic pulse receiver. The measurement was carried out three times on each material and arithmetic average values were specified. The contact angle measurement of epoxy nanocomposites was performed on Dataphysics Oca50Mikro to quantify degree of hydrophobicity. Bulk density of silica xerogel was calculated from mass to volume ratio. The density of each epoxy nanocomposite was calculated using Archimedes method. Water sorption of epoxy nanocomposites was investigated according to ASTM D 570 Standard. The water sorption percentage (M_t) was calculated using the following equation:

$$M_t\,(\%) = \left(\frac{m_t - m_0}{m_0}\right) x\ 100 \tag{1}$$

where m_t and m_0 (g) are mass of the material at time t and initial, respectively. The water sorption behavior of epoxy nanocomposites was determined using the following equation:

$$\frac{M_t}{M_\infty} = 4\left(\frac{Dt}{\pi h^2}\right)^{1/2} \tag{2}$$

where M_t and M_∞ are water sorption at time t and equilibrium point, respectively. D (mm^2/s) is diffusion coefficient and h (mm) is thickness of the material.

3. Results and discussion

3.1. Properties of silica xerogel

The FTIR spectrum of silica xerogel is shown in Fig. 1a. The peak attributed to O-Si-O bending vibration was observed at 459 cm^{-1}. While the symmetric stretching vibration of Si-O-Si bond was specified at 798 cm^{-1}, the characteristic peak at 1073 cm^{-1} was corresponded to asymmetric stretching vibration of Si-O-Si bond [33]. The peak at around 949 cm^{-1} indicated Si-OH and $Si\text{-}O^-$ stretching vibrations [34]. The broad band centered at 3600 cm^{-1} was related with -OH bond stretching vibration of silanol groups and adsorbed water on the surface. Similarly, it was clearly seen -OH bond bending vibration of adsorbed water at 1644 cm^{-1} [20,35]. The bands at 2914 cm^{-1} and 1384 cm^{-1} were assigned to C-H bonds [36].

The XRD pattern of silica xerogel is shown in Fig. 1b. No significant diffraction peaks were observed of the silica xerogel. The broad peak at around 22° can be explained with amorphous structure formation of silica xerogel [37].

The SEM image of silica xerogel is shown in Fig. 1c. It can be said that the distribution of silica xerogel particles were uniform with nano particle size [38]. The porous structure was ambiguously seen due to low resolution of SEM. And also, it can be expressed with irreversible shrinkage of the silica gel during the aging and ambient pressure drying [16].

The N_2 adsorption-desorption isotherm of silica xerogel is shown in Fig. 1d. The silica xerogel exhibited type IV adsorption isotherm which is characteristic property of mesoporous materials according to IUPAC classification. The hysteresis loop in the desorption cycle was closely associated with capillary condensation in the mesopores [39]. Besides, specific surface area of silica xerogel was determined as high as 252 $m^2/$

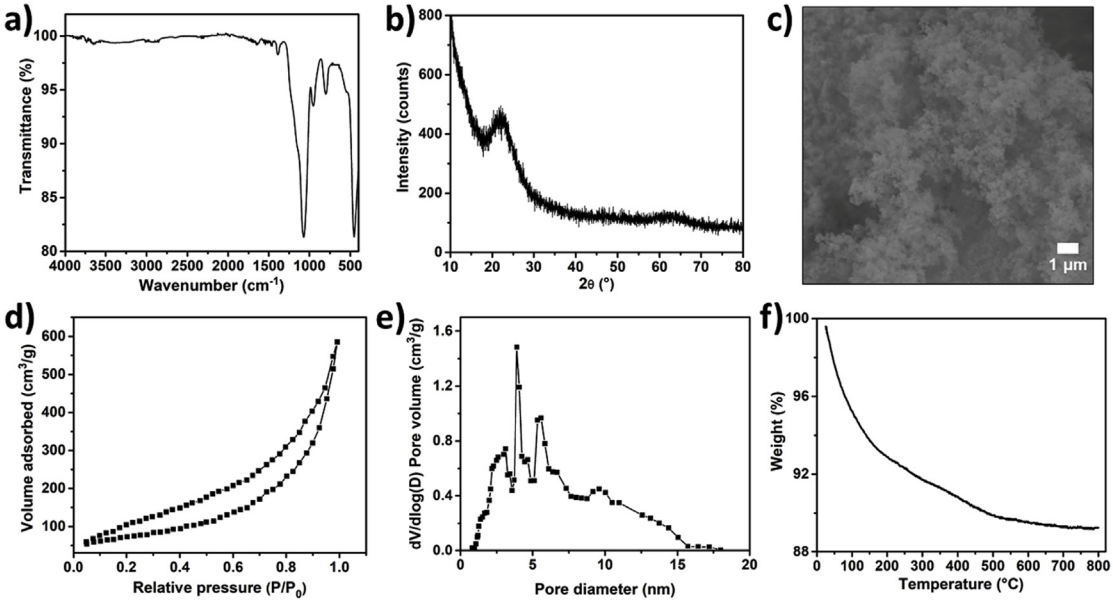

Fig. 1. a) FTIR spectrum, **b)** XRD pattern, **c)** SEM image, **d)** N_2 adsorption-desorption isotherm, **e)** pore size distribution and **f)** TGA curve of silica xerogel.

g.

The pore size distribution of silica xerogel is shown in Fig. 1e. Additionally, the pore structure properties of silica xerogel are given in Table 1 in details. It was obviously seen that pore diameter of the silica xerogel distributed between 1 nm and 18 nm with average pore diameter of 4 nm. Based on IUPAC consideration, the pores from 2 nm to 50 nm are classified as mesopores [40]. From this point of view, it can be said that the obtained silica xerogel was mesoporous material. The total volume of silica xerogel was specified as 0.90 cm^3/g.

The bulk density of the silica xerogel was 0.048 g/cm^3 that was considerably lower than many types of silica xerogel synthesized from ethyltrimethoxysilane (0.794 g/cm^3), methyltrimethoxysilane (0.089 g/cm^3) [41], tetraethoxysilane (0.680 g/cm^3) [42] in addition to cellulose (0.230 g/cm^3) [43], rice hull ash (1.250 g/cm^3) [44], kaolin (0.060 g/cm^3) [17] etc. in the literature.

The TGA curve of the silica xerogel is shown in Fig. 1f. The sharp weight loss up to 200 °C was related with evaporation of residual solvents and physically adsorbed water [39]. The thermal decomposition of organic groups caused a decrease in weight of silica xerogel between 200 °C and 600 °C [16]. Subsequently, the weight loss rate decreased and weight remained almost constant above 600 °C. The char residue at 800 °C was determined as approximately 89% which is desirable property in thermal stability required applications.

In spite of ambient pressure drying, the silica xerogel showed low thermal conductivity as well as 0.040 W/mK. Thermal conductivity was directly associated with density and pore structure of silica xerogel. Silica xerogels with smaller pore size than aerogels exhibit a less dependence on gas pressure and weaker dependence on temperature than low density aerogels because of higher density, so they may be an advantage in high temperature applications [45]. When compared to conventional thermal insulation materials such as mineral wool (0.034–0.045 W/mK), glass wool (0.031–0.043 W/mK), foam glass (0.038–0.050 W/mK), expanded polystyrene (0.029–0.055 W/mK), polyurethane foam (0.020–0.029 W/mK), silica aerogel (0.012–0.020 W/mK) [46], the obtained silica xerogel with low thermal conductivity had a great potential to replace traditional and expensive thermal insulators.

Table 1
Properties of silica xerogel.

Bulk density (g/cm^3)	BET surface area (m^2/g)	BJH pore volume (cm^3/g)	Average pore size (nm)	Thermal conductivity (W/mK)
0.048	252	0.900	4	0.040

3.2. Properties of silica xerogel/epoxy nanocomposites

The SEM images of the silica xerogel/epoxy nanocomposites are shown in Fig. 2. It can be seen from Fig. 2a that the surface of neat ER was smooth with river lines which is indication of brittleness. The morphology of nanocomposites became rougher in the presence of silica xerogels, as shown in Fig. 2b–c. The small amount of silica xerogel was uniformly dispersed in ER which results in good interfacial adhesion between filler and matrix [47]. However, agglomeration was observed with the addition of 1.5 wt% silica xerogel in Fig. 2d in line with morphology of epoxy nanocomposites including nano size fillers [48,49]. It can be explained with deficiency of filler modification. Since an increase in interaction between functional groups on the filler surface and matrix provided higher surface charge that leads homogeneous dispersion [50].

The TGA curves of the silica xerogel/epoxy nanocomposites are shown in Fig. 3. It was clear that the epoxy nanocomposites demonstrated a single weight loss step. Initial decomposition temperatures of the epoxy nanocomposites were considerably close each other at about 300 °C. The incorporation of silica xerogel had slight influence on the thermal stability of the epoxy nanocomposites in low temperatures. However, an increase in thermal decomposition temperatures of the epoxy nanocomposites was observed with the addition of silica xerogel above 430 °C. And also, the char residue of epoxy nanocomposites at 600 °C significantly increased with increasing amount of silica xerogel. The char residue of neat ER increased from 15.46% to 20.30% in the presence of 1.5 wt% silica xerogel. It can be corresponded to restriction of epoxy chains mobility due to silica xerogels and higher energy was necessary for the initiation of mobility that provided higher thermal stability of the nanocomposites [51].

It was clearly seen from Table 2 that thermal conductivity of neat ER decreased with silica xerogel addition. The thermal conductivity of neat ER was decreased from 0.260 W/mK to 0.220 W/mK with 1.5 wt% silica xerogel. By the help of three-dimensional mesoporous structure of silica xerogel as well as low density, heat transfer was decreased through neat ER. In other words, mesoporous network extends mean free path of heat transfer that can considerably reduce thermal

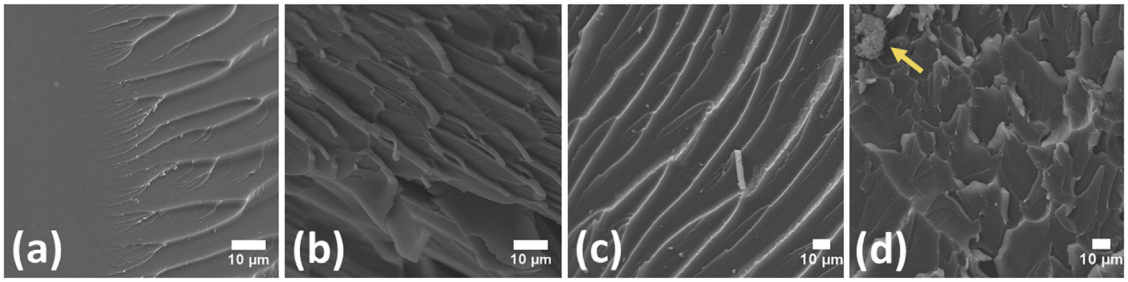

Fig. 2. SEM images of the silica xerogel/epoxy nanocomposites.

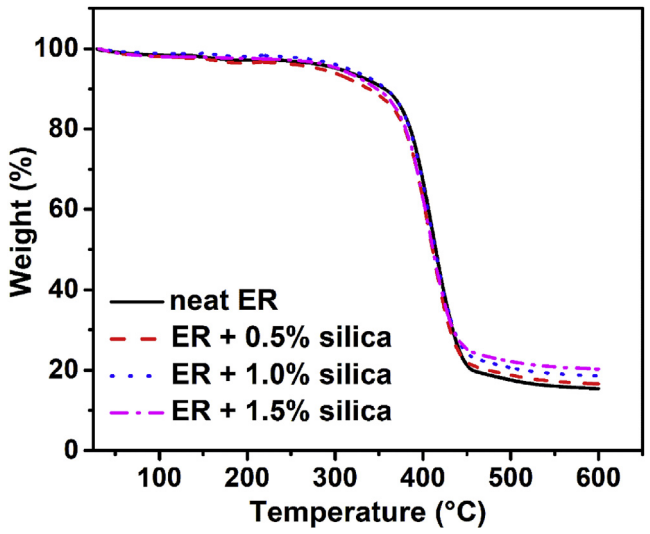

Fig. 3. TGA curves of the silica xerogel/epoxy nanocomposites.

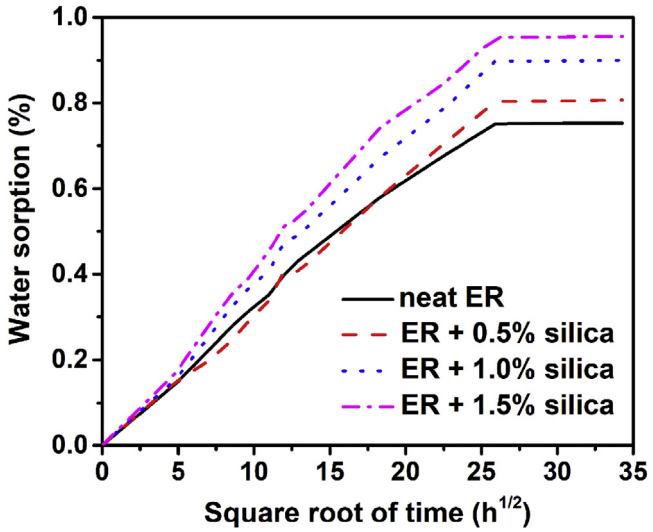

Fig. 4. Water sorption of the silica xerogel/epoxy nanocomposites.

conductivity of matrix. In the literature, similar trend has been observed about thermal conductivity of epoxy composites [52,53]. When considered the low thermal conductivity of silica xerogel/epoxy nanocomposites in this study, they can be regarded as potential thermal insulation material in many applications such as heat and cold storage devices, transport vehicles, roofs, laminates, flooring boards and windows, and so on [54].

Acoustic velocity of the neat ER decreased with the incorporation of silica xerogel as can be seen in Table 2. The mesoporous structure of the silica xerogel provided to decrease acoustic velocity of the epoxy nanocomposites. To make it clear, silica xerogel nanoparticles were effective in taking waves longer time to transfer through the epoxy nanocomposites. The lowest acoustic velocity was determined as 2372 m/s for epoxy nanocomposite including 1.5 wt% silica xerogel. It can be said that an increase in acoustic performance of this epoxy nanocomposite was related with agglomeration as well as mesoporous network [55]. The obtained acoustic velocity values were close to that of the studies in the literature [56,57].

It was observed from Table 2 that density of the epoxy nanocomposites were almost the same at around 1.20 g/cm^3. Addition of small amount of silica xerogel slightly affected density of the epoxy nanocomposites. So, the effect of density on the thermal and acoustic insulation properties of the epoxy nanocomposites was not investigated in details. The certain amount of low density filler addition to the neat ER generally decreases density; however applied force from the epoxy chains might lead to collapse filler pores which caused an increase in density of the materials [52].

The water sorption percentage of the silica xerogel/epoxy nanocomposites as a function of square root of time is shown in Fig. 4. In all epoxy composites, the water sorption continuously increased with immersion time until saturation level. Water sorption increased linearly in the initial step, and then slowed down towards equilibrium point which is described as typical Fickian diffusion behavior. The addition of 1.5 wt % silica xerogel increased water sorption percentage of the neat ER from 0.752% to 0.953% due to the mesoporous network of silica xerogel in addition to hydroxyl groups in the structure. The hydroxyl groups tend to combine with water molecules through hydrogen bonding [58]. In spite of an increase in water sorption, the water sorption percentage of the epoxy nanocomposites was below 1% which can be negligible for an epoxy nanocomposite. And also, maximum water diffusion coefficient was determined as 1.38×10^{-8} mm^2/s for the epoxy nanocomposite including 1.5 wt% silica xerogel. When examined many studies about water sorption of the epoxy nanocomposites in the literature, the obtained values were significantly low in this

Table 2
Properties of silica xerogel/epoxy nanocomposites.

Sample	Density (g/cm^3)	Thermal conductivity (W/mK)	Acoustic velocity (m/s)	Water diffusion coefficient (mm^2/s)
Neat ER	1.2075	0.260	2541	7.12×10^{-9}
ER + 0.5% silica	1.2086	0.240	2493	8.54×10^{-9}
ER + 1.0% silica	1.2087	0.230	2455	1.09×10^{-8}
ER + 1.5% silica	1.2088	0.220	2373	1.38×10^{-8}

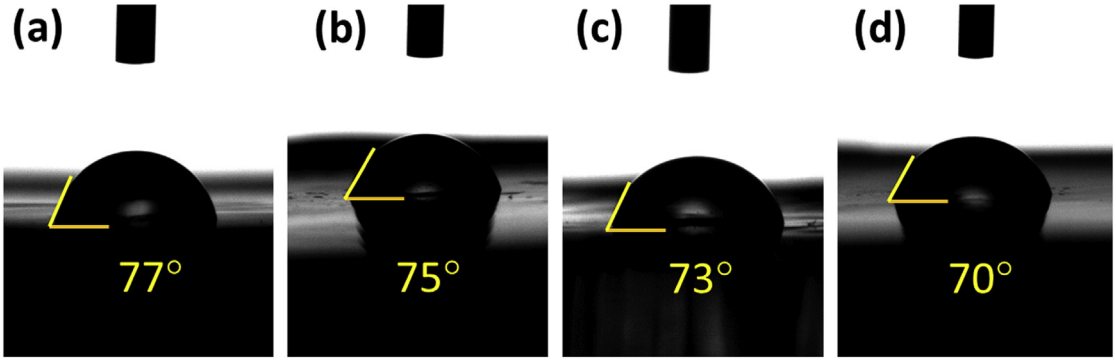

Fig. 5. Contact angles of the silica xerogel/epoxy nanocomposites.

study. Basri et al. [59] investigated water absorption performance of silica aerogel/epoxy nanocomposites and determined the lowest water absorption as 7.3%. Alamri and Low [60] indicated that the lowest water absorption was stated as 1.56% with the addition of 5 wt% nano-silicon carbide to the neat ER. Abdul Khalil et al. [61] prepared epoxy nanocomposites based on nano-structured oil palm ash. It was observed that the water absorption of neat ER increased to approximately 1.5% in case of 1 wt% filler content.

The contact angles of the silica xerogel/epoxy nanocomposites are shown in Fig. 5. The contact angle results were in line with water sorption values of the epoxy nanocomposites. The contact angle of neat ER slightly decreased with increasing amount of silica xerogel. The contact angle values of the epoxy nanocomposites were between 75° and 70° which is indication of hydrophilic surface. And also, wetting property of the surface significantly changes depending on surface roughness and surface energy of the materials. In the light of this information, smooth surface of the neat ER was highly effective to make nanocomposite surface hydrophilic [62].

4. Conclusion

In the present study, low cost and environmentally friendly silica xerogel from CSA was successfully synthesized by sol-gel method in ambient pressure drying. The low density (0.048 g/cm^3), mesoporous structure, high thermal stability and low thermal conductivity (0.040 W/mK) of the silica xerogel made it promising material for thermal and acoustic applications. When considered the attractive properties of the silica xerogel, silica xerogel in different weight ratios was used as filler in neat ER. The good interfacial adhesion between silica xerogel and neat ER was observed; however an agglomeration was determined in epoxy nanocomposite including 1.5 wt% silica xerogel. An increasing amount of silica xerogel in the neat ER not only provided to enhance thermal stability of the epoxy nanocomposites, but also decreased thermal conductivity of the materials due to the mesoporous structure and low density of silica xerogel. The acoustic velocity of the neat ER decreased from 2541 m/s to 2373 m/s in the presence of 1.5 wt% silica xerogel. The water sorption of the epoxy nanocomposites showed a slight increase with the addition of silica xerogel as well as water diffusion coefficient up to 0.95% and 1.38×10^{-8} mm^2/s, respectively. A general review, the silica xerogel synthesis with unique properties from agricultural waste in ambient pressure drying can be desirable for cost effective applications. And also, utilization of silica xerogel in neat ER most likely can make the epoxy nanocomposites suitable for many fields especially in thermal and acoustic insulation required.

Acknowledgements

The authors would like to thank to the Academic Staff Training Program (Project Number: 2016-ÖYP-071), TÜBITAK for 2211-E Direct PhD Scholarship Programme, and Selcuk University Scientific Research Foundation.

References

[1] Asdrubali F, D'Alessandro F, Schiavoni S. A review of unconventional sustainable building insulation materials. Sustain Mater Technol 2015;4:1–17.
[2] Baetens R, Jelle BP, Gustavsen A. Aerogel insulation for building applications: a state-of-the-art review. Energy Build 2011;43:761–9.
[3] Jelle BP. Traditional, state-of-the-art and future thermal building insulation materials and solutions – properties, requirements and possibilities. Energy Build 2011;43:2549–63.
[4] Zhou X, Carmeliet J, Derome D. Influence of envelope properties on interior insulation solutions for masonry walls. Build Environ 2018;135:246–56.
[5] Koebel M, Rigacci A, Achard P. Aerogel-based thermal superinsulation: an overview. J Sol Gel Sci Technol 2012;63:315–39.
[6] Rasmussen B, Rindel JH. Sound insulation between dwellings – descriptors applied in building regulations in Europe. Appl Acoust 2010;71:171–80.
[7] Choe H, Sung G, Kim JH. Chemical treatment of wood fibers to enhance the sound absorption coefficient of flexible polyurethane composite foams. Compos Sci Technol 2018;156:19–27.
[8] Cotana F, Pisello AL, Moretti E, Buratti C. Multipurpose characterization of glazing systems with silica aerogel: in-field experimental analysis of thermal-energy, lighting and acoustic performance. Build Environ 2014;81:92–102.
[9] Sehaqui H, Zhou Q, Berglund LA. High-porosity aerogels of high specific surface area prepared from nanofibrillated cellulose (NFC). Compos Sci Technol 2011;71:1593–9.
[10] Huang WF, Tsui GCP, Tang CY, Yang M. Fabrication and process investigation of vancomycin loaded silica xerogel/polymer core–shell composite nanoparticles for drug delivery. Compos B Eng 2016;95:272–81.
[11] Hrubesh LW. Aerogel applications. J Non-Cryst Solid 1998;225:335–42.
[12] Li H, Song L, Fu Y, Wei Y, Li R, Liu H. Loads transfer across static electrical phase interfaces in silica aerogel/polymethyl methacrylate composites. Compos Sci Technol 2017;138:169–78.
[13] Madyan OA, Fan M, Feo L, Hui D. Enhancing mechanical properties of clay aerogel composites: an overview. Compos B Eng 2016;98:314–29.
[14] Kim HM, Kim HS, Kim SY, Youn JR. Silica aerogel/epoxy composites with preserved aerogel pores and low thermal conductivity. E-Polymers 2015;15(2):111–7.
[15] Shi F, Liu J-X, Song K, Wang Z-Y. Cost-effective synthesis of silica aerogels from fly ash via ambient pressure drying. J Non-Cryst Solid 2010;356:2241–6.
[16] Gao G-M, Liu D-R, Zou H-F, Zou L-C, Gan S-C. Preparation of silica aerogel from oil shale ash by fluidized bed drying. Powder Technol 2010;197:283–7.
[17] Hu W, Li M, Chen W, Zhang N, Li B, Wang M. Preparation of hydrophobic silica aerogel with kaolin dried at ambient pressure. Colloid Surface A Physicochem Eng Asp 2016;501:83–91.
[18] Wu W, Wang K, Zhan M-S. Preparation and performance of polyimide-reinforced clay aerogel composites. Ind Eng Chem Res 2012;51:12821–6.
[19] Li A, Lin R, Lin C, He B, Zheng T, Lu L. An environment-friendly and multi-functional absorbent from chitosan for organic pollutants and heavy metal ion. Carbohydr Polym 2016;148:272–80.
[20] Fu J, Wang S, He C, Lu Z, Huang J, Chen Z. Facilitated fabrication of high strength silica aerogels using cellulose nanofibrils as scaffold. Carbohydr Polym 2016;147:89–96.
[21] Nazriati N, Setyawan H, Affandi S, Yuwana M, Winardi S. Using bagasse ash as a silica source when preparing silica aerogels via ambient pressure drying. J Non-Cryst Solid 2014;400:6–11.
[22] Aripin H, Mitsudo S, Prima ES, Sudiana IN, Kikuchi H, Sano S. Crystalline mullite formation from mixtures of alumina and a novel material—silica xerogel converted from sago waste ash. Ceram Int 2015;4:6488–97.
[23] Ubeyitogullari A, Ciftci ON. Formation of nanoporous aerogels from wheat starch. Carbohydr Polym 2016;147:125–32.
[24] Qu Y, Tian Y, Zou B, Zhang J, Zheng Y, Wang L. A novel mesoporous lignin/silica hybrid from rice husk produced by a sol-gel method. Bioresour Technol 2010;101:8402–5.

[25] Lou C, Liu X. Functional dendritic curing agent for epoxy resin: processing, mechanical performance and curing/toughening mechanism. Compos B Eng 2018;136:20–7.
[26] Sangermano M, D'Anna A, Marro C, Klikovits N, Liska R. UV-activated frontal polymerization of glass fibre reinforced epoxy composites. Compos B Eng 2018;143:168–71.
[27] Liu S, Chevali VS, Xu Z, Hui D, Wang H. A review of extending performance of epoxy resins using carbon nanomaterials. Compos B Eng 2018;136:197–214.
[28] Xu Y-J, Wang J, Tan Y, Qi M, Chen L, Wang Y-Z. A novel and feasible approach for one-pack flame-retardant epoxy resin with long pot life and fast curing. Chem Eng J 2018;337:30–9.
[29] Chen S, Xu Z, Zhang D. Synthesis and application of epoxy-ended hyperbranched polymers. Chem Eng J 2018;343:283–302.
[30] Kalapathy U, Proctor A, Shultz J. A simple method for production of pure silica from rice hull ash. Bioresour Technol 2000;73:257–62.
[31] Tang Q, Wang T. Preparation of silica aerogel from rice hull ash by supercritical carbon dioxide drying. J Supercrit Fluids 2005;35:91–4.
[32] Oral I, Guzel H, Ahmetli G, Gur CH. Determining the elastic properties of modified polystyrenes by sound velocity measurements. J Appl Polym Sci 2011;121:3425–32.
[33] Abdul Halim ZA, Mat Yajid MA, Hamdan H. Synthesis and characterization of rice husk ash derived - silica aerogel beads prepared by ambient pressure drying. Key Eng Mater 2016;694:106–10.
[34] Li M, Jiang H, Xu D, Hai O, Zheng W. Low density and hydrophobic silica aerogels dried under ambient pressure using a new co-precursor method. J Non-Cryst Solid 2016;452:187–93.
[35] Al-Oweini R, El-Rassy H. Synthesis and characterization by FTIR spectroscopy of silica aerogels prepared using several $Si(OR)_4$ and $R''Si(OR')_3$ precursors. J Mol Struct 2009;919:140–5.
[36] Wörmeyer K, Alnaief M, Smirnova I. Amino functionalised Silica-Aerogels for CO_2-adsorption at low partial pressure. Adsorption 2012;18:163–71.
[37] Affandi S, Setyawan H, Winardi S, Purwanto A, Balgis R. A facile method for production of high-purity silica xerogels from bagasse ash. Adv Powder Technol 2009;20:468–72.
[38] Durães L, Ochoa M, Rocha N, Patrício R, Duarte N, Redondo V. Effect of the drying conditions on the microstructure of silica based xerogels and aerogels. J Nanosci Nanotechnol 2012;12:6828–34.
[39] Hilonga A, Kim J-K, Sarawade PB, Kim HT. Low-density TEOS-based silica aerogels prepared at ambient pressure using isopropanol as the preparative solvent. J Alloy Comp 2009;487:744–50.
[40] Ślosarczyk A, Wojciech S, Piotr Z, Paulina J. Synthesis and characterization of carbon fiber/silica aerogel nanocomposites. J Non-Cryst Solid 2015;416:1–3.
[41] Ochoa M, Durães L, Beja AM, Portugal A. Study of the suitability of silica based xerogels synthesized using ethyltrimethoxysilane and/or methyltrimethoxysilane precursors for aerospace applications. J Sol Gel Sci Technol 2011;61:151–60.
[42] Fidalgo A, Ilharco LM. The influence of the wet gels processing on the structure and properties of silica xerogels. Microporous Mesoporous Mater 2005;84:229–35.
[43] Han Y, Zhang X, Wu X, Lu C. Flame retardant, heat insulating cellulose aerogels from waste cotton fabrics by in situ formation of magnesium hydroxide nanoparticles in cellulose gel nanostructures. ACS Sustainable Chem Eng 2015;3:1853–9.
[44] Kalapathy U, Proctor A, Shultz J. Silica xerogels from rice hull ash: structure, density and mechanical strength as affected by gelation pH and silcia concentration. J Chem Technol Biotechnol 2000;75:464–8.
[45] Einarsrud M-A, Haereid S, Wittwer V. Some thermal and optical properties of a new transparent silica xerogel material with low density. Sol Energy Mater Sol Cell 1993;31:341–7.
[46] Cuce E, Mert Cuce P, Wood CJ, Riffat SB. Toward aerogel based thermal superinsulation in buildings: a comprehensive review. Renew Sustain Energy Rev 2014;34:273–99.
[47] Wu Z, Gao S, Chen L, Jiang D, Shao Q, Zhang B, Zhai Z, Wang C, Zhao M, Ma Y, Zhang X, Weng L, Zhang M, Guo Z. Electrically insulated epoxy nanocomposites reinforced with synergistic core-shell SiO_2@MWCNTs and monymorillonite bi-fillers. Macromol Chem Phys 2017;218:1700357.
[48] Zare Y. Study of nanoparticles aggregation/agglomeration in polymer particulate nanocomposites by mechanical properties. Composer Part A Appl Sci Manufact 2016;84:158–64.
[49] Fu J, Shi L, Zhang D, Zhong Q, Chen Y. Effect of nanoparticles on the performance of thermally conductive epoxy adhesives. Polym Eng Sci 2010;50:1809–19.
[50] Ab Rahman I, Padavettan V. Synthesis of silica nanoparticles by sol-gel: size-dependent properties, surface modification, and applications in silica-polymer nanocomposites-a review. J Nanomater 2012;2012:132424.
[51] Poh CL, Mariatti M, Ahmad Fauzi MN, Ng CH, Chee CK, Chuah TP. Tensile, dielectric, and thermal properties of epoxy composites filled with silica, mica, and calcium carbonate. J Mater Sci Mater Electron 2014;25:2111–9.
[52] Maghsoudi K, Motahari S. Mechanical, thermal, and hydrophobic properties of silica aerogel-epoxy composites. J Appl Polym Sci 2018;135:45706.
[53] Zhao J, Ge D, Zhang S, Wei X. Studies on thermal property of silica aerogel/epoxy composite. Mater Sci Forum 2007;546–549:1581–4.
[54] He Y-L, Xie T. Advances of thermal conductivity models of nanoscale silica aerogel insulation material. Appl Therm Eng 2015;81:28–50.
[55] Oral I, Soydal U, Bentahar M. Ultrasonic characterization of andesite waste-reinforced composites. Polym Bull 2016;74:1899–914.
[56] Oral I. Determination of elastic constants of epoxy resin/biochar composites by ultrasonic pulse echo overlap method. Polym Compos 2016;37:2907–15.
[57] Oral I. Ultrasonic characterization of conductive epoxy resin/polyaniline composites. J Appl Polym Sci 2015;132:42748.
[58] Wan YZ, Luo H, He F, Liang H, Huang Y, Li XL. Mechanical, moisture absorption, and biodegradation behaviours of bacterial cellulose fibre-reinforced starch biocomposites. Compos Sci Technol 2009;69:1212–7.
[59] Basri MSM, Mazlan N, Mustapha F. Effects of stirring speed and time on water absorption performance of silica aerogel/epoxy nanocomposites. J Eng Appl Sci 2015;10(21):9982–91.
[60] Alamri H, Low IM. Effect of water absorption on the mechanical properties of nanofiller reinforced epoxy nanocomposites. Mater Des 2012;42:214–22.
[61] Abdul Khalil HPS, Fizree HM, Bhat AH, Jawaid M, Abdullah CK. Development and characterization of epoxy nanocomposites based on nano-structured oil palm ash. Compos B Eng 2013;53:324–33.
[62] Kang Y, Chen X, Song S, Yu L, Zhang P. Friction and wear behavior of nanosilica-filled epoxy resin composite coatings. Appl Surf Sci 2012;258:6384–90.